

# Infrared radiation generated by quasi-phase-matched difference-frequency mixing in a periodically poled lithium niobate waveguide

E. J. Lim, H. M. Hertz,<sup>a)</sup> M. L. Bortz, and M. M. Fejer  
*Edward L. Ginzton Laboratory, Stanford University, Stanford, California 94305*

(Received 14 June 1991; accepted for publication 26 August 1991)

We report quasi-phase-matched difference-frequency generation of 2.1  $\mu\text{m}$  radiation at room temperature using the  $d_{33}$  nonlinear coefficient in a periodically poled lithium niobate channel waveguide. A tunable Ti:Al<sub>2</sub>O<sub>3</sub> laser ( $\lambda \approx 0.8 \mu\text{m}$ ) and a Nd:YAG laser ( $\lambda = 1.32 \mu\text{m}$ ) were the pump and signal sources, respectively. With 160 mW of 0.81  $\mu\text{m}$  and 1 mW of 1.32  $\mu\text{m}$  radiation coupled into the waveguide, 1.8  $\mu\text{W}$  of 2.1  $\mu\text{m}$  radiation was generated, tunable over a 6 nm bandwidth. We also show that the annealed proton exchange process can change the shape of ferroelectric domains in lithium niobate.

Coherent sources of infrared radiation in the wavelength range of 2–4  $\mu\text{m}$  are required for applications such as spectroscopy, sensors, infrared fibers, and laser radar. Although laser sources exist in this spectral region, guided-wave difference-frequency mixing<sup>1–3</sup> of near-infrared diode lasers offers the possibility of achieving milliwatt power levels of mid-infrared radiation in a compact, room-temperature device. This letter reports the application of periodically poled lithium niobate (LiNbO<sub>3</sub>) waveguides to the generation of coherent 2.1  $\mu\text{m}$  radiation by room-temperature, quasi-phase-matched, difference-frequency mixing of 0.81 and 1.32  $\mu\text{m}$  laser radiation.

Parametric interactions for infrared generation previously demonstrated in LiNbO<sub>3</sub> waveguide devices include difference-frequency generation<sup>1–3</sup> (DFG) and optical parametric oscillation.<sup>4</sup> These devices employed birefringent phase matching using the  $d_{31}$  nonlinear coefficient, used dye lasers in the visible or color center lasers in the 1.45–1.6  $\mu\text{m}$  range as pump sources, and required phase-matching temperatures of 200–400 °C. To use pump sources such as near-infrared diode lasers in the 0.8–0.9  $\mu\text{m}$  range, birefringently phase-matched interactions would require even higher phase-matching temperatures.<sup>3</sup> Quasi-phase matching, however, allows the use of 0.8–0.9  $\mu\text{m}$  pump sources in these parametric interactions at more convenient temperatures.

Quasi-phase matching (QPM), an early proposal for compensating refractive-index dispersion in nonlinear optics, involves modulating the nonlinear coefficient of the medium every coherence length  $l_c$  of the interaction.<sup>5</sup> For quasi-phase matched guided-wave DFG, the phasematching requirement is

$$\Delta\beta = \beta_p - \beta_s - \beta_i - 2\pi/\Lambda \approx 0, \quad (1)$$

where  $\Delta\beta$  is the phase mismatch,  $\Lambda$  is the period of the modulation of the nonlinear coefficient where  $\Lambda = 2l_c$ , and  $\beta$  is the propagation constant of the optical waveguide mode, where the subscripts  $p$ ,  $s$ , and  $i$  in this and following equations identify the pump, signal, and idler frequencies ( $\omega_p$ ,  $\omega_s$ , and  $\omega_i$ ), respectively, which are related by  $\omega_p$

$= \omega_s + \omega_i$ . QPM enables the use of the largest nonlinear coefficient of LiNbO<sub>3</sub>,  $d_{33}$ , and allows phase matching at room temperature.

In ferroelectrics, the signs of the nonlinear coefficients are linked to the direction of the spontaneous electric polarization, and thus QPM can be accomplished through periodic ferroelectric domain reversal. This technique has been applied in LiNbO<sub>3</sub> to second-harmonic generation of visible radiation in bulk<sup>6–8</sup> and guided-wave<sup>9,10</sup> geometries. Previous workers discovered that ferroelectric domain reversal can accompany titanium diffusion into the +Z face of LiNbO<sub>3</sub> plates<sup>11</sup> and applied this effect to acoustic devices.<sup>12</sup> We have combined the Ti-diffusion method of patterning the ferroelectric domains with an annealed proton exchange waveguide process to fabricate waveguide doublers<sup>9</sup> and the difference frequency mixer reported here.

To periodically pole the substrate, we indiffuse a grating of Ti lines, where, using the extraordinary refractive indices for bulk LiNbO<sub>3</sub>,<sup>13</sup> the grating period  $\Lambda$  is about 21  $\mu\text{m}$  for a DFG interaction in which  $\lambda_p = 0.81 \mu\text{m}$ ,  $\lambda_s = 1.32 \mu\text{m}$ , and  $\lambda_i = 2.1 \mu\text{m}$ . We defined the grating of 5- $\mu\text{m}$ -wide Ti lines with period  $\Lambda = 21 \mu\text{m}$  on the +Z surface of a 1-mm-thick, integrated optics-grade, Z-cut LiNbO<sub>3</sub> substrate with lift-off lithography. The Ti lines had a thickness of 5 nm and were parallel to the Y axis of the crystal. The Ti grating was then diffused into the substrate with a 2 h ramp-up from room temperature to 1100 °C and a 2 h soak at 1100 °C, after which the oven was turned off and allowed to cool to room temperature with an initial cooling rate of 8 K/min. To prevent outdiffusion of lithium oxide from the sample during the poling process, the substrate was placed in a closed alumina boat filled with congruent lithium niobate powder.<sup>14</sup> Figure 1(a) shows a polished and etched Y face of a Z-cut LiNbO<sub>3</sub> substrate following the indiffusion of the Ti grating, illustrating the resulting triangular, reversed domains. Preferential etching in HF was used to reveal the reversed domains.<sup>15</sup>

After the heat treatment, annealed proton exchange (APE) channel waveguides were fabricated in the substrate.<sup>16</sup> Channels parallel to the X axis, with widths in the range 2–15  $\mu\text{m}$ , were defined in a 200-nm-thick layer of

<sup>a)</sup>Present address: Department of Physics, Lund Institute of Technology, Lund, Sweden.

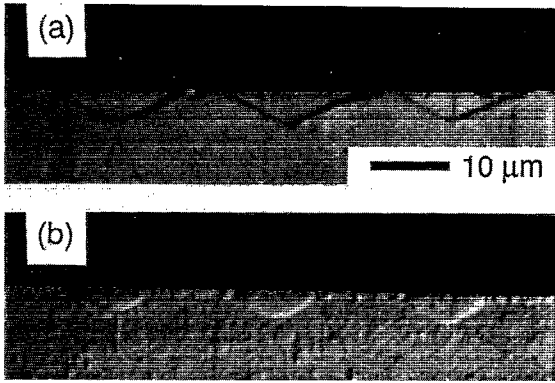


FIG. 1. Photomicrographs of polished and etched Y faces of a planar, periodically poled Z-cut LiNbO<sub>3</sub> substrates (a) after indiffusion of the Ti grating, showing the triangular shape of the reversed domains, and (b) after the annealed proton exchange process, showing the rounding of the domains. In both photographs the period of the pattern is 21  $\mu\text{m}$ .

aluminum on the substrate using lift-off lithography. Following a 2 h soak in pure benzoic acid at 200  $^{\circ}\text{C}$ , the Al mask was removed in a solution of NaOH. The sample was then annealed in air for 12 h at 333  $^{\circ}\text{C}$ . Figure 1(b) shows the polished and etched cross section of a periodically poled sample after an unmasked APE process, where we see that the process has changed the shape of the triangular domains, rounding them but not significantly reducing their depth.

For the optical experiment, pump radiation in the 0.8–0.9  $\mu\text{m}$  range from a cw tunable Ti:Al<sub>2</sub>O<sub>3</sub> laser and signal radiation at 1.32  $\mu\text{m}$  from a cw Nd:YAG laser were endfire coupled into a 5- $\mu\text{m}$ -wide waveguide on a 7-mm-long sample as shown in Fig. 2. For a pump wavelength of  $\lambda_p = 0.81 \mu\text{m}$ , difference-frequency output at  $\lambda_i = 2.1 \mu\text{m}$  was detected after a germanium filter with a lead sulfide detector and a lock-in amplifier. Several modes at 0.81  $\mu\text{m}$  and the lowest-order mode at 1.3  $\mu\text{m}$  were observed, and the waveguide was assumed to be single moded at 2.1  $\mu\text{m}$ . All modes were TM, and thus were coupled by the  $d_{33}$  coefficient. Figure 3 shows the idler power increasing linearly with pump power, as expected in a low-gain interaction. A maximum of 1.8  $\mu\text{W}$  of 2.1  $\mu\text{m}$  idler radiation was measured with 160 mW of 0.81  $\mu\text{m}$  and 1 mW of 1.32  $\mu\text{m}$  radiation coupled into the waveguide. Figure 4 shows the

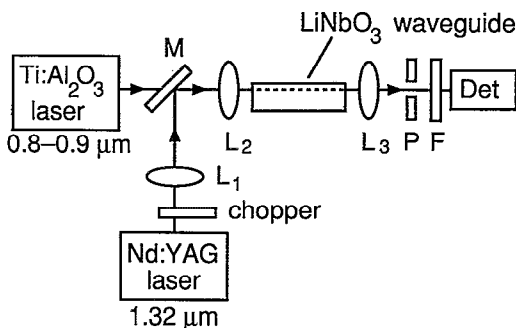


FIG. 2. Experimental setup:  $L_1$ – $L_3$ , lenses;  $M$ , dichroic mirror;  $P$ , pinhole;  $F$ , Ge filter;  $\text{Det}$ , PbS photoconductive detector.

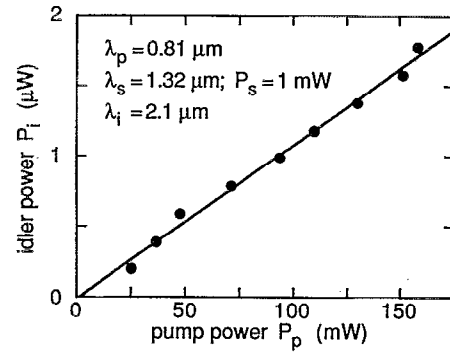


FIG. 3. Linear dependence of the measured difference-frequency power at 2.1  $\mu\text{m}$  on pump power.

difference-frequency power as a function of pump wavelength. The observed power at the difference frequency as a function of pump wavelength. The observed full width at half maximum (FWHM) pump wavelength tuning bandwidth, 0.86 nm, corresponds to a tuning bandwidth of 5.8 nm for the idler wavelength.

From the bulk refractive indices for LiNbO<sub>3</sub>,<sup>13</sup> the theoretical FWHM pump bandwidth is calculated to be 4.5 nm mm. The observed FWHM in Fig. 4 thus implies an effective interaction length of about 5 mm, in reasonable agreement with the 7 mm device length. Together with the power levels given earlier, this results in an experimental normalized conversion efficiency of about 4%/W cm<sup>2</sup>.

In the limit of small conversion efficiency the power  $P_i$  at the difference frequency is given by

$$P_i = \eta_{\text{nor}} P_p P_s L^2, \quad (2)$$

where  $P$  denotes power,  $L$ , the interaction length, and  $\eta_{\text{nor}}$ , the normalized efficiency that accounts for the material and geometrical aspects of the device: the overlap of the modes, the nonlinear coefficient, and the effective nonlinear coefficient determined by the implementation of QPM. This figure of merit is given by<sup>17–19</sup>

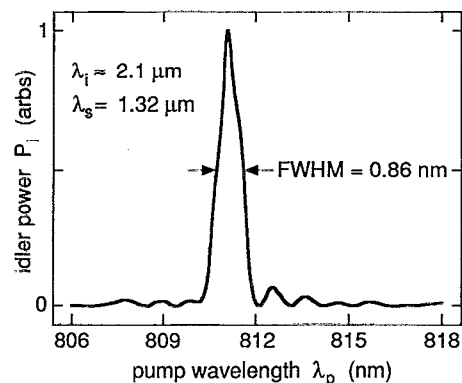


FIG. 4. Measured difference-frequency power at about 2.1  $\mu\text{m}$  vs pump wavelength. The 0.86 nm FWHM bandwidth of the pump wavelength corresponds to a tuning bandwidth in the idler wavelength of 5.8 nm.

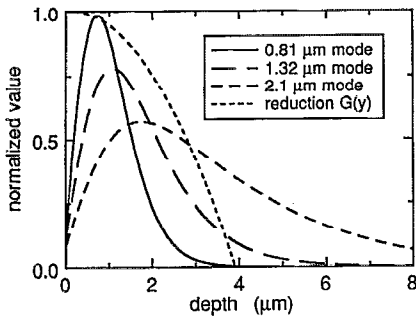


FIG. 5. Calculated normalized mode depth profiles along with the nonlinear coefficient reduction factor  $G(y)$  as defined in Eq. (4).

$$\eta_{\text{nor}} = \left( \frac{4}{\pi^2} \right) \frac{8\pi^2 d_{33}^2}{N_p N_s N_i c \epsilon_0 \lambda_i^2} \left| \int_{-\infty}^{+\infty} \int_{-\infty}^{+\infty} G(y) E_p(x, y) \times E_s(x, y) E_i(x, y) dx dy \right|^2, \quad (3)$$

where the factor  $(4/\pi^2)$  is the reduction of the effective nonlinear coefficient that arises from the use of first-order QPM,<sup>20</sup>  $N$  is the modal effective index,  $c$  is the vacuum speed of light,  $\epsilon_0$  is the vacuum permittivity,  $\lambda_i$  is the idler wavelength,  $x$  and  $y$  are the channel waveguide width and depth coordinates, respectively,  $E$  is the normalized modal electric field distribution, and  $G(y)$  is a function that describes the reduction in the effective nonlinear coefficient when the modulation of the nonlinear coefficient varies with depth, as it does in our device as shown in Fig. 1. The reduction factor  $G(y)$  in this case is the normalized Fourier coefficient of the spatial frequency of the modulation that accomplishes QPM,

$$G(y) = \frac{1}{2} [1 - \cos(\pi l(y)/l_c)], \quad (4)$$

where  $l(y)$  is the length of the reversed domain at depth  $y$ . We see that  $G(y)$  is unity for perfect, 50% duty cycle modulation [ $l(y) = l_c$ ] and falls to zero when there is no modulation [ $l(y) = 0$  or  $l(y) = 2l_c$ ].

To estimate the overlap integral in our device, we have, from the waveguide fabrication parameters given earlier, derived the modal distributions in the depth shown in Fig. 5 using a one-dimensional nonlinear diffusion model.<sup>21</sup> Also in Fig. 5 we show the reduction factor  $G(y)$  as estimated from the profile of the domains in Fig. 1(b). It is fortuitous that the maxima and minima of  $G(y)$  and the pump mode nearly coincide, as this reduces the deleterious effect of the nonideally shaped domains on the overlap integral. Evaluating the integral results in an effective depth of  $7.1 \mu\text{m}$ . Assuming a flat top lateral dimension of  $5 \mu\text{m}$  gives an effective area of about  $36 \mu\text{m}^2$ . This results in a predicted normalized efficiency of  $95\%/W \text{ cm}^2$ , about 24 times larger than the measured efficiency. We attribute the difference to one or more of the following: the reduction of  $d_{33}$  that accompanies proton exchange,<sup>22-24</sup> the

launching of pump radiation into higher-order modes which have substantially smaller overlap integrals, and inadequate modeling of the lateral diffusion of the APE process.

In conclusion, we have demonstrated infrared generation of  $2.1 \mu\text{m}$  radiation in a  $\text{LiNbO}_3$  waveguide by quasi-phase-matched, room-temperature, difference-frequency mixing of two wavelengths that can be provided by diode lasers:  $0.81$  and  $1.32 \mu\text{m}$ . Further work in this field should produce compact, diode-laser-pumped guided-wave difference-frequency devices or optical parametric oscillators, providing milliwatt levels of tunable mid-infrared radiation.

We are grateful to D. Sipes of Amoco Laser Company for loaning us the Nd:YAG laser, to T. Kubo of Lightwave Electronics for loan of equipment, to Crystal Technology, Inc. for providing the  $\text{LiNbO}_3$  substrates, to G. Woods for assistance in the characterization of the device, and to T. Carver, L. Goddard, K. Goesele, and J. Vrhel for assistance in fabrication. We acknowledge support from the Joint Services Electronics Program.

- <sup>1</sup>N. Uesugi, Appl. Phys. Lett. **36**, 178 (1980).
- <sup>2</sup>W. Sohler and H. Suche, Appl. Phys. Lett. **37**, 255 (1980).
- <sup>3</sup>H. Herrmann and W. Sohler, J. Opt. Soc. Am. B **5**, 278 (1988).
- <sup>4</sup>H. Suche and W. Sohler, Optoelectronics **4**, 1 (1989).
- <sup>5</sup>J. A. Armstrong, N. Bloembergen, J. Ducuing, and P. S. Pershan, Phys. Rev. **127**, 1918 (1962).
- <sup>6</sup>D. Feng, N. Ming, J. Hong, Y. Yang, J. Zhu, Z. Yang, and Y. Wang, Appl. Phys. Lett. **37**, 607 (1980).
- <sup>7</sup>A. Feisst and P. Koidl, Appl. Phys. Lett. **47**, 1125 (1985).
- <sup>8</sup>G. A. Magel, M. M. Fejer, and R. L. Byer, Appl. Phys. Lett. **56**, 108 (1990).
- <sup>9</sup>E. J. Lim, M. M. Fejer, and R. L. Byer, Electron. Lett. **25**, 174 (1989).
- <sup>10</sup>J. Webjorn, F. Laurell, and G. Arvidsson, IEEE Photon. Technol. Lett. **1**, 316 (1989).
- <sup>11</sup>S. Miyazawa, J. Appl. Phys. **50**, 4599 (1979).
- <sup>12</sup>K. Nakamura, H. Ando, and H. Shimizu, in *1986 Ultrasonics Symposium Proceedings*, edited by B. R. McAvoy (IEEE, New York, 1986), p. 719.
- <sup>13</sup>G. J. Edwards and M. Lawrence, Opt. Quantum Electron. **16**, 373 (1984).
- <sup>14</sup>R. L. Holman, in *Processing of Crystalline Ceramics*, edited by H. Palmour, R. F. Davis, and T. M. Hare (Plenum, New York, 1978), p. 343.
- <sup>15</sup>N. Nüzeki, T. Yamada, and H. Toyoda, Jpn. J. Appl. Phys. **6**, 318 (1967).
- <sup>16</sup>P. G. Suchoski, T. K. Findakly, and F. J. Leonberger, Opt. Lett. **13**, 1050 (1988).
- <sup>17</sup>M. M. Fejer, G. A. Magel, and E. J. Lim, in *Nonlinear Optical Properties of Materials*, edited by H. R. Schlossberg and R. V. Wick, Proc. SPIE **1148**, 213 (1989).
- <sup>18</sup>B. Jaskorzynska, G. Arvidsson, and F. Laurell, Proc. SPIE **651**, 221 (1986).
- <sup>19</sup>R. L. Byer, in *Nonlinear Optics*, edited by P. G. Harper and B. S. Wherrett (Academic, San Francisco, 1977), p. 47.
- <sup>20</sup>J. D. McMullen, J. Appl. Phys. **46**, 3076 (1975).
- <sup>21</sup>M. L. Bortz and M. M. Fejer, Opt. Lett. (to be published).
- <sup>22</sup>T. Sahara, H. Tazaki, and H. Nishihara, Electron. Lett. **25**, 1328 (1989).
- <sup>23</sup>R. W. Keys, A. Loni, and R. M. De La Rue, Electron. Lett. **26**, 624 (1990).
- <sup>24</sup>X. Cao, R. Srivastava, R. V. Ramaswamy, and J. Natour, IEEE Photon. Technol. Lett. **3**, 25 (1991).